END
DATE
FILMED
82
DTIC

MICROCOPY RESOLUTION TEST CHART

NATIONAL BUREAU OF STANDARDS 1963 A

LEVEL $\overline{II}$

MICROSTRUCTURAL SOURCES OF TOUGHNESS IN QLT-TREATED 5.5 Ni CRYOGENIC STEEL

By

J. I. Kim, C. K. Syn and J.W. Morris, Jr.

Department of Materials Science and Engineering
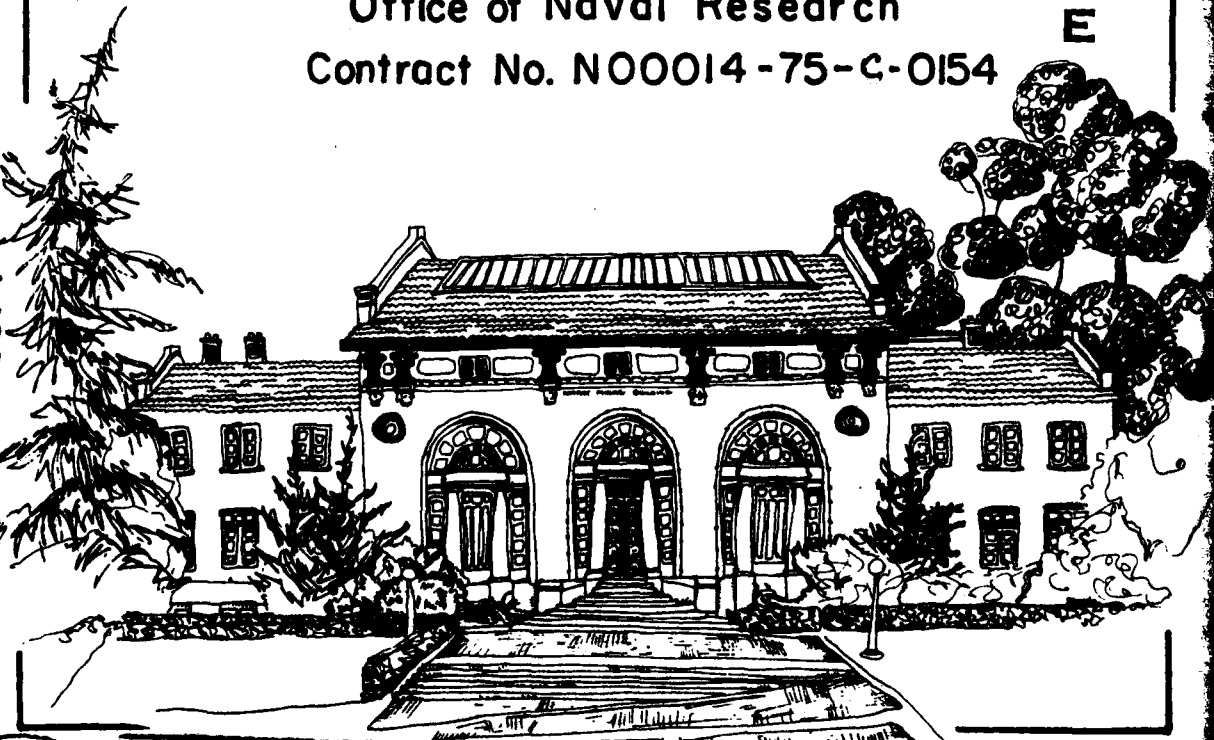
University of California, Berkeley

AD A109616

DTIC
ELECTE
JAN 15 1982
S
E

DTIC FILE COPY

81 12 14 072

REPORT DOCUMENTATION PAGE	READ INSTRUCTIONS BEFORE COMPLETING FORM	
1. REPORT NUMBER 11	2. GOVT ACCESSION NO. AD-A109 616	3. RECIPIENT'S CATALOG NUMBER •
4. TITLE (and Subtitle) MICROSTRUCTURAL SOURCES OF TOUGHNESS IN QLT-TREATED 5.5Ni CRYOGENIC STEEL	5. TYPE OF REPORT & PERIOD COVERED Technical Report, 1981	
	6. PERFORMING ORG. REPORT NUMBER	
7. AUTHOR(s) J.I. Kim, C.K. Syn and J. W. Morris, Jr. Dept. of Materials Science University of California, Berkeley	8. CONTRACT OR GRANT NUMBER(s) N00014-75-C-0154	
9. PERFORMING ORGANIZATION NAME AND ADDRESS	10. PROGRAM ELEMENT, PROJECT, TASK AREA & WORK UNIT NUMBERS	
11. CONTROLLING OFFICE NAME AND ADDRESS Office of Naval Research Metallurgy and Ceramics Program	12. REPORT DATE September, 1981	
	13. NUMBER OF PAGES 20	
14. MONITORING AGENCY NAME & ADDRESS(If different from Controlling Office)	15. SECURITY CLASS. (of this report) Unclassified	
	15a. DECLASSIFICATION, DOWNGRADING SCHEDULE	

16. DISTRIBUTION STATEMENT (of this Report)

> This document has been approved for public release and sale; its distribution is unlimited.

17. DISTRIBUTION STATEMENT (of the abstract entered in Block 20, if different from Report)

18. SUPPLEMENTARY NOTES

19. KEY WORDS (Continue on reverse side if necessary and identify by block number)

Cryogenic mechanical properties, 5.5 Ni steel, Heat treatment, Tempering Retained Austenite

20. ABSTRACT (Continue on reverse side if necessary and identify by block number)

In commercial practice 5.5Ni steel is toughened for cryogenic service by a three-step heat treatment designated the "QLT" treatment. To determine why this treatment is necessary and successful, a series of two-step heat treatments were applied to 5.5Ni steel and the resulting microstructural states were characterized and compared with that resulting from the QLT treatment. It was concluded from this analysis that the QLT treatment lowers the ductile-brittle transition essentially be refining the grain size of the alloy through (Cont.)

DD FORM 1473 JAN 73   EDITION OF 1 NOV 65 IS OBSOLETE

S/N 0102 LF 014 6601

ABSTRACT (Cont.)

precipitation of thermally stable austenite in a dense distribution
along the boundaries of prior martensite laths, hence destroying the
crystallographic alignment of martensite packets and preventing co-
operative cleavage. The multi-step heat treatment is necessary be-
cause of the low nickel content; a single step heat treatment leads
to an austenite precipitate which is either too lean in solute to be
retained or too coarse in its distribution to be effective. The
problem is avoided in the QLT treatment since the L intercritical
anneal serves to create regions of high solute content along the prior
martensite lath boundaries, and the intercritical temper, T, then pre-
cipitates a dense distribution of high solute, stable austenite within
these enriched regions.

A

INTRODUCTION

Ferritic steels which are intended for structural use at cryogenic temperatures are thermally processed to lower the ductile-brittle transition temperature to below the intended temperature of service. In conventional 9%Ni steel this treatment involves a straightforward intercritical temper at a relatively low temperature within the two-phase ($\alpha + \gamma$) region. During the intercritical temper a fine, dense distribution of austenite phase is precipitated along the boundaries of the dislocated laths of the martensite structure. The austenite is thermally stable on cooling to at least 77K. It apparently toughens the steel by breaking up the packet alignment of the martensite laths through a toughening mechanism described in reference 1.

Ferritic steels of lower nickel content can also be toughened for cryogenic service (2,3) as can ferritic iron-manganese steels containing no nickel at all (4,5). But in these cases more elaborate thermal treatments are required. The most commercially important of these alternative heat treatments is the so-called QLT treatment, which is a 3-step heat treatment employed for toughening the 5-6Ni steels developed some years ago by the Nippon Steel Corporation in Japan and by Armco Steel in the United States. The QLT treatment is the fourth of those diagrammed in Fig. 1. It involves two sequential intercritical heat treatments after initial quenching. The first of these (L) is an intercritical anneal in the upper range of the two-phase ($\alpha + \gamma$) field. The second (T) is an intercritical temper at lower temperature within the two-phase field.

While the QLT treatment has been used with commercial success for some years, the fundamental reasons for its effectiveness remains somewhat

unclear. The present research was undertaken to clarify the microstructural sources of toughening through this heat treatment. In previous papers we discussed the dominant mechanism by which a distribution of precipitated austenite lowers the ductile-brittle transition of ferritic steel (1), and determined the approximate composition of the precipitated austenite in Nippon 5.5Ni steel as a function of heat treatment, including the QLT treatment (6). In the work reported below we studied the interplay of composition and microstructure in determining the ductile-brittle transition temperature of 5.5Ni steel, with particular emphasis on the benefit achieved from the QLT treatment.

2. EXPERIMENTAL PROCEDURE

The alloy used for this investigation was a commercial Fe-5.5Ni steel which was provided by the Nippon Steel Corporation. Its composition was determined to be: Fe-5.86Ni-1.21Mn-0.69Cr-0.20Mo-0.2Si-0.06C-0.01S-0.08P (in wt.%). The as-received alloy was annealed at 1200°C for 2 hours to remove the effect of prior thermomechnical treatments. The alloy was then solution-annealed at 900°C for 2 hours. Experimental samples for microstructural analysis and mechanical testing were cut from the annealed plates and subjected to one of the four heat treatments diagrammed in Fig. 1. Each of these heat treatments begins with a treatment labelled Q, which involves austenization at 800°C for 1 hour followed by rapid quenching in ice water. Subsequent intercritical tempering at 600°C for 2 hours yields the treatment QT_2. Intercritical tempering at 600°C for 100 hours gives QT_{100}. Intercritical annealing at 670°C for 1 hour yields the treatment labelled QL. The QL treatment followed by an intercritical temper at 600°C for 1 hour gives the treatment labelled QLT. In all cases the samples are

quenched in ice water after heat treatment.

The microstructure of the alloys was studied as a function of heat treatment using optical, transmission and scanning transmission electron microscopy. The latter technique was used primarily to gain information about the chemical composition of the austenite present in the final structure. The details and results of this analysis are reported elsewhere (6).

The volume fraction of precipitated austenite was determined by x-ray diffraction using FeK_α radiation. For quantitative analysis the (220) and (311) austenite peaks were compared with the (211) martensite peak in the technique suggested by Miller (7). The volume fraction of precipitated austenite was determined both in specimens quenched to room temperature and in specimens which had been soaked in liquid nitrogen. The austenite fraction was also determined by backscatter Mössbauer spectroscopy using the apparatus and techniques described by Fultz (8). The Mössbauer measurements were used to calibrate the x-ray determinations and to identify the residual austenite in the surfaces of broken fracture specimens.

The mechanical property measurements included the yield strength and impact toughness. Yield strength was measured at room temperature and at 77K. The impact toughness was measured over a range of temperature to determine the ductile-brittle transition temperature. The impact tests employed standard Charpy V-notch specimens prepared according to ASTM specifications (9). Fractographic analyses of the broken Charpy V-notch test specimens included scanning electron fractographic studies and measurements of the residual austenite content through backscatter Mössbauer spectroscopy.

3. RESULTS

A. The Variation of Microstructure with Heat Treatment.

When a sample of Fe-5.5Ni steel is heated into the two-phase $(\alpha+\gamma)$ region, it undergoes a partial retransformation to austenite. If the holding temperature is not too high, the austenite precipitation is accomplished by diffusional processes, with the consequence that the chemical composition of the precipitated austenite differs from that of the residual ferrite. On subsequent quenching a portion of this precipitated austenite may retransform martensitically. The final microstructure will then be a mixture of three constituents: tempered martensite, which represents that part of the alloy which did not retransform on heating; fresh martensite, which represents that part of the precipitated austenite which retransforms during cooling; and austenite, which represents that part of the precipitated austenite which is retained. The martensite and austenite phases can be distinguished from one another through crystallographic measurements, such as dark-field transmission electron microscopy, or magnetic measurements, such as Mössbauer spectroscopy. The fresh and tempered martensites can often be distinguished from one another through differences in microstructure. The separation is sometimes clear, but is never entirely unambiguous. The microstructural changes which result from heat treatment involve changes in the size, shape, distribution, and volume fractions of these three constituents and in their internal composition and structure.

1. The Q Condition.

Figures 2 and 3 show the microstructure of the Fe-5.5Ni alloy in the reference or Q condition. Figure 2 is an optical micrograph. It

reveals a lath martensite structure in which martensite laths are organized into aligned packets which subdivide the prior austenite grains. Figure 3 is a transmission electron micrograph of the interior of a packet within this structure. The martensite is heavily dislocated. The accompanying diffraction pattern, which was taken from a region encompassing several laths, is a clean pattern of the BCC phase. The martensite laths tend to be in a single variant separated by small-angle lath boundaries.

2. The QT_2 Microstructure.

The microstructure of the alloy in the QT_2 condition is illustrated in Figs. 4, 5, and 6. Its austenite content after quenching to room temperature and after subsequent refrigeration at 77K is given in Table 1. The approximate content of substitutional alloying species within this austenite is presented in Table 2. The carbon content is not given since carbon is not detected in STEM.

The optical micrograph, Fig. 4, suggests that the QT_2 microstructure has a very fine grain size, with a mean grain diameter near 1 micron. Figure 5 reveals the source of this apparent grain refinement and suggests that it is spurious. The fine grains correspond to a polygonized structure within the tempered martensite. Electron diffraction patterns taken from region "A" in the micrograph, which includes several of these polygonized grains, and from region "B", which includes several grains and a part of a precipitated austenite particle, show that the α grains have an essentially constant orientation; the polygonized grains are separated by low-angle grain boundaries.

The austenite in the QT_2 structure is retained in relatively low volume fraction in the form of thin, lens-shaped particles, as shown in

Figs. 5 and 6 (the particles labelled austenite in this figure were iden-
tified by dark field electron microscopy). The austenite forms along the
boundaries of the martensite laths, and has the Kurdjumov-Sachs relation
to the parent martensite in each of the few cases which were specifically
analyzed. Just as the martensite adopts one crystallographic variant within
a packet, at least to within a very small rotation or tilt across the low-
angle lath boundaries, the austenite precipitated within a single packet
also forms in one predominant variant; the austenite particles give rise
to a single set of austenite diffraction spots and can be simultaneously
illuminated in a single dark field transmission electron micrograph. As
shown in Table 2, this austenite is relatively lean in substitutional solute
content. Its low solute content and small volume fraction are apparently
due to a combination of the low tempering temperature, the relatively short
tempering time, and the small diffusivity of the substitutional species
which preferentially segregate to the austenite phase. The low solute
content is presumably responsible for the thermal instability of this aus-
tenite; as shown in Table 1, the bulk of it reverts to martensite on cool-
ing to 77K.

3. The QT_{100} Microstructure.

Increasing the tempering time to 100 hours gives rise to the sub-
structure illustrated in Fig. 7. The tempered martensite retains a fine,
polygonized substructure, though the matrix dislocation density appears to
have decreased and the size of the polygonized subgrains to have increased
slightly. The austenite is present in much higher volume fraction, and
the precipitated austenite particles have coarsened and spheroidized into
more nearly equiaxed grains of approximately 0.5μ diameter. As shown in

Table 2, this austenite is much richer in substitutional solute content. It is also much more stable on quenching and is almost entirely retained after the sample has been cooled in liquid nitrogen.

4. The QL microstructure.

Increasing the heat treatment temperature to 670°C for 1 hour leads to the QL microstructure which is pictured in Fig. 8. The three separate constituents of this microstructure are apparent and are labelled in the figure. The regions labelled "F" are tempered martensite and have a fine, polygonized structure which resembles that of the martensite in the QT_2 microstructure. The regions labelled "M" contain fresh martensite which presumably arises from the retransformation of the greater part of the austenite precipitated during intercritical annealing. The STEM analysis (6) shows that this martenstie has essentially the same composition as the residual austenite. The regions labelled "A" in the figure are the retained portion of the precipitated austenite. The composition of this austenite is rich relative to that of the austenite retained after the QT_2 treatment, which presumably reflects its denser distribution and the greater diffusivity of the substitutional species at 670°C. This austenite is, however, unstable with respect to martensitic transformation on cooling (Table 1), which is probably due to its still low substitutional solute content (compare QT_{100} and QLT) and to a lower carbon content. The diffusivity of carbon is sufficiently high that carbon should equilibrate at the level appropriate to the temperature and the current solute content of the austenite; the austenite produced by the T treatment at 600°C should, therefore, be richer in carbon than that produced by the L treatment at 670°C.

The apparent "memory" exhibited by the transformations associated with the QL treatment is striking and significant. We have already noted that a given martensite racket tends to precipitate a single austenite variant on

heating. When this austenite retransforms it has a strong tendency to
reconstitute the martensite variant which gave it birth. This
phenomena is documented in Fig. 9, which shows a substructure of a QL sam-
ple after refrigeration at 77K. Both the polygonized structure of tempered
martensite and the dislocated structure of fresh martensite are apparent in
the bright field micrograph. The diffraction pattern is, however, very
nearly the clean pattern of a single BCC crystal, which shows that, at least
to within a small rotation across low-angle boundaries, the single variant
packet has been reformed.

5. The QLT microstructure.

When the QL treatment is followed by a temper at 600°C for 1 hour,
the result is the QLT treatment. The microstructure of the steel after
this heat treatment (Fig. 10) consists of three constituents whose origin
may be seen from the schematic diagram of the transformation sequence pre-
sented in Fig. 11. The L treatment causes a chemical decomposition of the
alloy into regions which are relatively rich or relatively poor in solute
content. The subsequent T treatment causes a secondary decomposition of
the solute-rich islets. The final microstructure consists of a low solute
tempered martensite matrix containing elongated regions of solute-rich
tempered martensite which themselves contain elongated subregions of high-
solute precipitated austenite with a slight admixture of fresh martensite.
The austenite phase is shown in the dark field micrograph in Fig. 10. Its
composition (Table 2) is very nearly equal to that of the austenite formed
after 100 hours tempering at 600°C. Virtually all of this austenite is
retained on refrigeration at 77K (Table 1).

B. The Variation of Mechanical Properties with Heat Treatment.

Table 3 shows typical tensile properties of the alloy in the QLT con-
dition at room temperature and at 77K. Since the tensile properties do not
change greatly with heat treatment, these are representative of the tensile

properties of the alloys of all four conditions. The toughness of the alloy was measured by determining its Charpy impact energy as a function of temperature. The results are plotted in Fig. 12. The most evident changes include the dramatic increase in the upper shelf Charpy energy on tempering the initial Q alloy, and the dramatic decrease in the ductile-brittle transition temperature in the QLT condition.

Figure 13 shows the appearance of the fracture surface at 77K as a function of heat treatment. The ductile rupture mode of the QLT specimen is contrasted to the cleavage or quasi-cleavage fracture apparent on the surfaces of the specimens in the other three conditions.

4. DISCUSSION

A. Relation of Toughness to Microstructure.

Previous research suggests that intercritical heat treatment influences the toughness of ferritic cryogenic steels primarily because of the precipitation and retention of the austenite phase. The precipitation of austenite can affect both the level of toughness above the ductile-brittle transition and the value of the ductile-brittle transition temperature (10).

The level of toughness above the ductile-brittle transition temperature is influenced by intercritical heat treatment when the base alloy contains carbon (as do, for example, commercial 9Ni and 5-6Ni steels) but is usually not affected when the alloy is carbon-free or carbon-gettered. The major source of toughening is believed to be the gettering of carbon from the martensite matrix through its segregation to the precipitated austenite. Even if most of the precipitated austenite retransforms, as it does after the QL treatment, the carbon remains largely confined to the regions of the lattice which previously transformed to austenite, with the consequence

that most of the increment to toughness is retained.

The ductile-brittle transition temperature usually decreases after intercritical heat treatment. The dominant contribution to this behavior appears to be the grain refining effect of the precipitated austenite, which is somewhat subtle. As shown in Fig. 14, the brittle fracture of ferritic cryogenic steel in the as-quenched condition occurs through progressive cleavage primarily along the (100) cleavage planes of the α-martensite matrix. Because of the crystallographic alignment of adjacent laths within a martensite packet, potential cleavage planes often traverse the packet, as shown in Fig. 2, with the consequence that the martensite packet size acts as the effective grain size for transgranular cleavage fracture. The precipitation of austenite along the martensite lath boundaries serves to divide up the cleavage planes, as illustrated in Fig. 15, and hence refines the effective grain size of the alloy. But this grain refinement is indirect. In virtually all cases studied to date the precipitated austenite is mechanically unstable and is transformed to martensite by the plastic deformation associated with the advancing crack. But the crystallographic variant of the martensite product is influenced by the mechanical state at the time of transformation; as illustrated in Fig. 16, the martensite variant adopted by the mechanically retransformed austenite is usually different from the dominant variant of the surrounding packet. The crystallographic alignment of the martensite packet is hence broken up, and the possibility of clean trans-packet cleavage along the crystallographic planes is removed.

Since the ductile-brittle transition is associated with the replacement of ductile rupture by the cleavage fracture mode, microstructural changes which increase the difficulty of cleavage fracture are effective in lowering the ductile-brittle transition temperature.

These considerations suggest that the critical element in the microstructure of an intercritically-tempered ferritic cryogenic steel is the distribution of precipitated austenite, and that to establish low temperature toughness the precipitated austenite should have two characteristics: it should have sufficient thermodynamic stability to resist transformation under mechanical load until its preferred variant is decoupled from that of the surrounding packet, and it should be present in a sufficiently dense distribution that unperturbed trans-packet cleavage paths are uncommon. The thermomechanical stability of the precipitated austenite depends primarily upon its chemical composition, as documented in Tables 1 and 2, though there are indications that the state of strain of austenite may also play a role (11). The distribution of the austenite depends on a balance between its nucleation and growth kinetics, and on the total tempering time.

B. The Relation of Microstructure to Processing.

If the objective of thermal processing in 5.5Ni steel is to achieve a dense distribution of stable austenite, then the QLT treatment is well designed. The low nickel content of the alloy and the slow diffusion kinetics of substitutional species, such as nickel, which stabilize austenite, make it very difficult to achieve a desirable microstructure with a single tempering treatment. If the alloy is tempered at relatively low temperature, as in the QT_2 treatment, then the precipitated austenite is lean in

solute content and is thermally unstable. Its thermal instability may be overcome by increasing the tempering time to raise the solute content, as in the QT_{100} treatment, but in this case the austenite particles become blocky and widely separated. It is then relatively easy to locate trans-packet cleavage which avoids the austenite entirely. If the heat treatment temperature is raised, as in the QL treatment, then a dense distribution of austenite particles is precipitated. But in this case also the austenite is relatively lean in solute content and is thermally unstable. The QLT treatment avoids these difficulties by precipitating the final austenite from within the solute-rich regions within the microstructure, as shown schematically in Fig. 11.

The austenite precipitated during the T-step of the QLT treatment is rich in solute since it forms within L-product regions that are themselves rich in solute. The austenite is fine in size and dense in distribution since the L-product regions are densely distributed through the microstructure along the boundaries of the initial martensite laths. The fine distribution is retained since only a short tempering time is required to establish both the distribution and stability of the austenite, and very little particle coarsening occurs.

In effect, the QLT treatment is a means for "tricking" the microstructure into behaving as if it had a much higher nickel content. The nickel content of the L-product regions is very near 9wt.% (Table 1). The kinetics of austenite precipitation during the final temper, and its stability and distribution bear a strong resemblance to those observed in tempered 9Ni steel.

C. Implications for Other Alloys.

The observations reported here suggest that the successful heat treatments of Fe-Ni ferritic cryogenic steels can be rationalized, and new and improved heat treatments sought, from a perspective which asserts that the primary objective of the heat treatment is to create a dense distribution of thermally stable austenite, that austenite stability is controlled primarily by its composition, and that one can best achieve a favorable combination of austenite stability and distribution by insuring that the austenite forms from a solute-rich matrix. In 9 and 12Ni cryogenic steels, the initial matrix is itself sufficiently rich in solute to permit the dense decoration of martensite lath boundaries with a high solute stable austenite. In 5-6Ni steels the matrix must first be conditioned by an intercritical anneal which serves the function of plating high solute regions along the martensite laths, which then act as a template for subsequent precipitation of a dense distribution of stable austenite.

If this reasoning holds, it should be possible to achieve good low temperature properties in alloys of still lower nickel content by tailoring the heat treatment to create high solute regions along the lath boundaries prior to the final tempering step. Researchers at the Central Research Laboratories of Nippon Kokan KK (12) have, in fact, recently reported excellent cryogenic properties in the 3.5-4Ni range following a heat treatment which they labelled QQ'Q"T. While the relevant chemical analysis has not yet been done, it seems likely that this two-step intermediate treatment serves precisely the function of enriching the martensite lath boundaries to permit subsequent precipitation of a dense distribution of stable austenite.

-14-

5. CONCLUSION

We conclude from the work reported here that a multi-step heat treatment is necessary to impart low temperature toughness to 5-6Ni steels through the austenite precipitation mechanism. The QLT treatment is a suitable multi-step heat treatment for this purpose. This heat treatment lowers the ductile-brittle transition essentially by refining the grain size of the alloy through precipitation of thermally stable austenite in a dense distribution along the boundaries of prior martensite laths, hence destroying the crystallographic alignment of martensite packets and preventing cooperative cleavage. The multi-step heat treatment is necessary because of the low nickel content; a single step heat treatment leads to an austenite precipitate which is either too lean in solute to be retained or too coarse in its distribution to be effective. The problem is avoided in the QLT treatment since the L intercritical anneal serves to create regions of high solute content along the prior martensite lath boundaries, and the intercritical temper, T, then precipitates a dense distribution of high solute, stable austenite within these enriched regions.

REFERENCES

1. J. W. Morris, Jr., C. K. Syn, J. I. Kim and B. Fultz; Proceedings of the International Conference on Martensitic Transformation, 1979, MIT, Cabridge, MA., p. 572.

2. S. Nagashima, T. Ooka, S. Sekino, H. Mimura, T. Fujishima, S. Yano, and H. Sakurai; Trans. ISIJ, 1971, vol. 11, p. 402.

3. S. Nagashima, T. Ooka, S. Sekino, H. Mimura, T. Fujishima, S. Yano, and H. Sakurai; Tetsu-to-Hagane, 1972, vol. 58, p. 128.

4. M. Niikura and J. W. Morris, Jr.; Met. Trans. A, 1980, vol. 11A, p. 1531.

5. S. K. Hwang and J. W. Morris, Jr.; Met. Trans. A, 1980, vol. 11A, p. 1197.

6. J. I. Kim and J. W. Morris, Jr.; in press in Met. Trans. A.

7. R. L. Miller; Trans. ASM, 1964, 57, p. 892.

8. B. Fultz; M.S. Thesis, University of California, Berkeley, 1978.

9. ASTM Standard E 23, Annual Book of ASTM Standards, 1979, p. 237.

10. J. I. Kim and J. W. Morris, Jr.; Met. Trans. A, 1980, vol. 11A, p. 1401.

11. B. Fultz, J. I. Kim and J. W. Morris, Jr.; unpublished research.

12. M. Niikura, Central Research Laboratories, Nippon Kokan, K.K., private communication.

TABLE 1: Volume percent of the retained austenite at 298°K and at 77°K.

	298°K	77°K
QT_2	5.9	3.8
QT_{100}	8.2	7.9
QL	8.8	2.0
QLT	9.2	8.8

TABLE 2: Composition of the retained austenite analyzed by scanning transmission electron microscopy; given in wt.%.

	Fe	Ni	Mn	Cr	Si
QT_2	89.5	6.6	2.2	1.2	0.1
QT_{100}	85.0	9.1	3.8	1.5	0.2
QL (γ)	86.1	8.4	3.7	1.3	0.1
(α')	86.7	8.2	3.4	1.1	0.1
QLT	82.8	8.8	4.3	3.2	0.5

TABLE 3: Tensile property of QLT-treated Fe-5.5Ni alloy at 298°K and at 77°K.

	298°K	77°K
Y.S (Ksi)	93.8	126.3
U.T.S. (Ksi)	118.0	173.7
R. A. (%)	75.0	77.5
Total elongation (%)	32.2	35.3

FIGURE CAPTIONS

1. Schematic diagram of 4 heat treatments.

2. Optical micrograph showing the as-quenched microstructure. Arrows indicate the probable crack propagation inhibiting sites.

3. Transmission electron micrograph of as-quenched microstructure and accompanying diffraction pattern taken from a region encompassing several laths.

4. Optical micrograph of the alloy after the QT_2 treatment described in the text.

5. Transmission electron micrograph of the alloy after the QT_2 treatment. The diffraction patterns A and B are taken from the regions A and B in the bright field, respectively.

6. Transmission electron micrograph of the alloy after the QT_2 treatment: (a) bright field and (b) dark field of the retained austenite.

7. Transmission electron micrograph of the alloy after the QT_{100} treatment.

8. Transmission electron micrograph of the alloy after the QL treatment. The letters M, F, and A indicate fresh martensite, the ferrite (tempered martensite) matrix, and the retained austenite, respectively.

9. Transmission electron micrograph of the alloy after the QL heat treatment showing the orientation of the thermally transformed austenite (i.e. martensite), which is the same as that of the ferrite matrix.

10. Transmission electron micrograph of the alloy after the QLT heat treatment. Figure B shows the dark field of the retained austenite.

11. Schematic diagram of the transformation sequence during the QT_2 and QLT treatments. The letters A and M denote the retained austenite and the martensite, repectively.

12. The Charpy impact energy of the Fe-5.5Ni alloy as a function of heat treatment and temperature.

13. Fractographs of the specimens broken at 77K: (a) QT_2 specimen, (b) QT_{100} specimen, (c) QL specimen, and (d) QLT specimen.

14. Transmission electron micrograph of the cross-section of a broken Charpy specimen of Fe-9Ni in the as-quenched condition. The fracture surface was Fe-plated.

15. Transmission electron micrograph of a quenched-and-tempered 9Ni alloy and a dark field image of the stable retained austenite.

16. Transmission electron micrograph of a 3% strained quenched and tempered 9Ni steel: (a) bright field, (b) dark field of mechanically transformed martensite, and (c) dark field of the retained austenite which still remained. The letters T.A. indicate the direction of the tensile axis.

20 μm

Figure 1

Figure 2

0.5μm
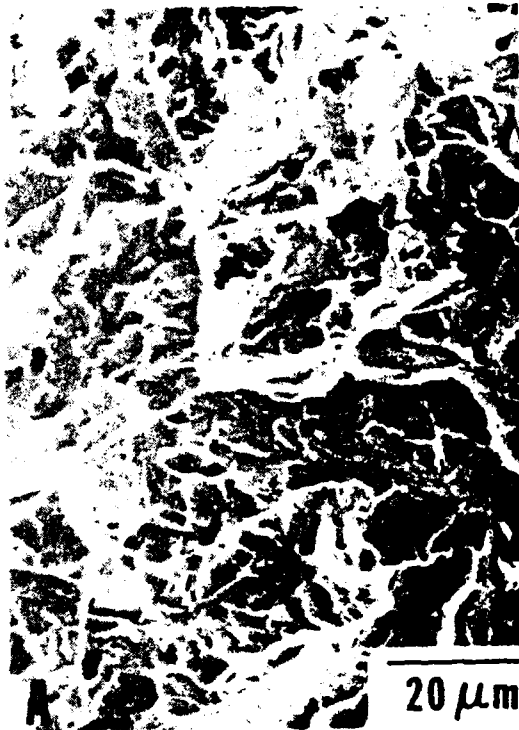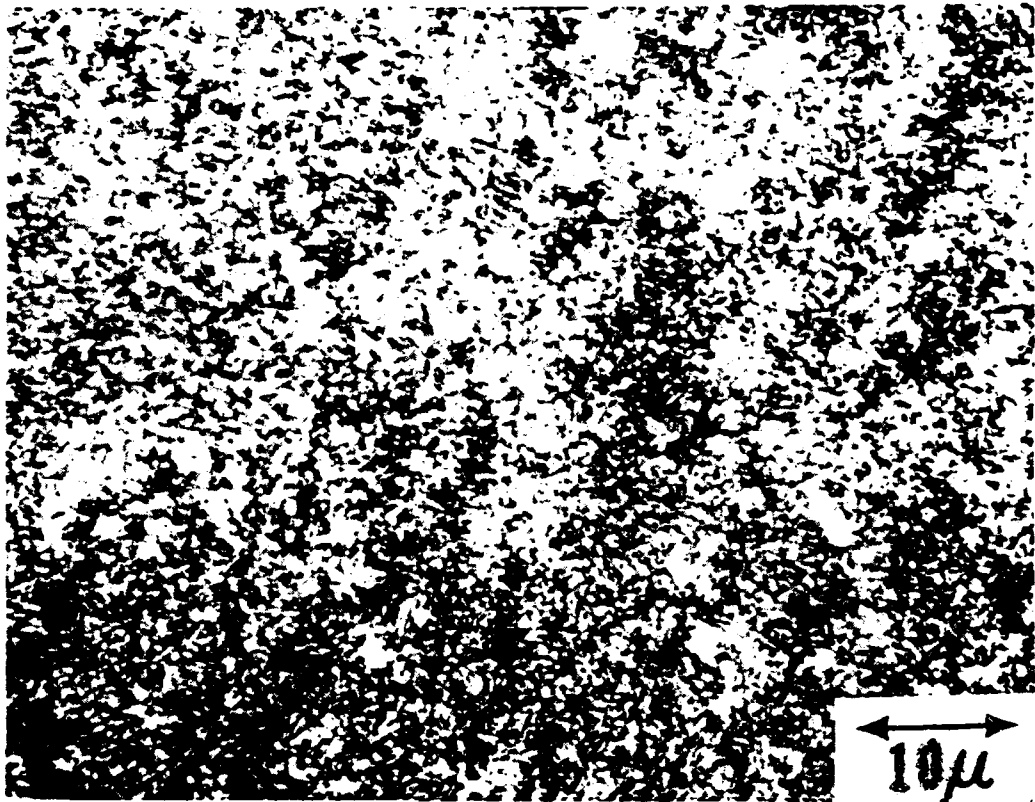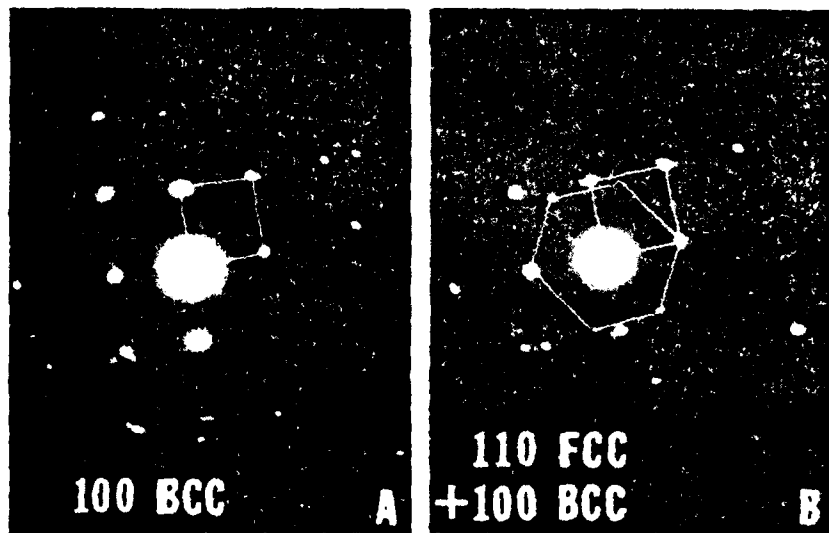
Figure 3

Figure 4

Figure 5
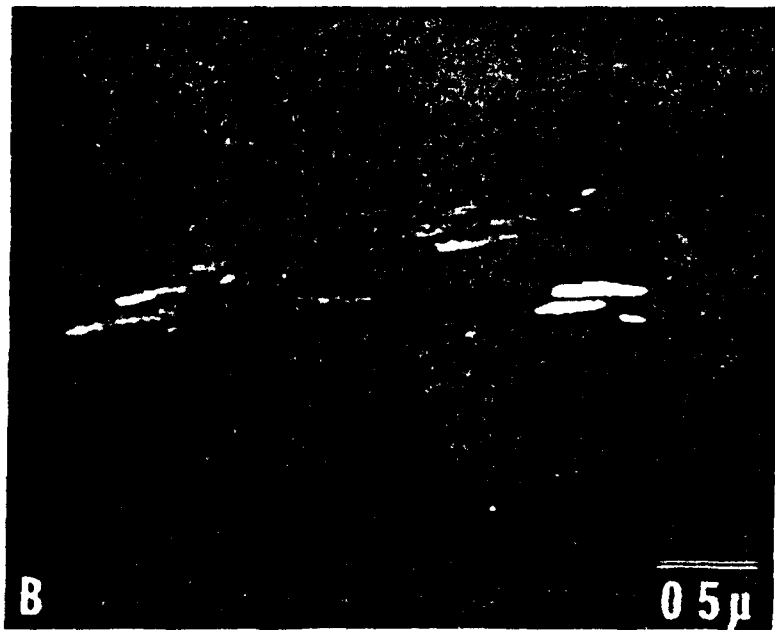
Figure 6

Figure 7

Figure 8

(110)

(100)

0.4μ

(020)

(1̄10)

(200)

(110)
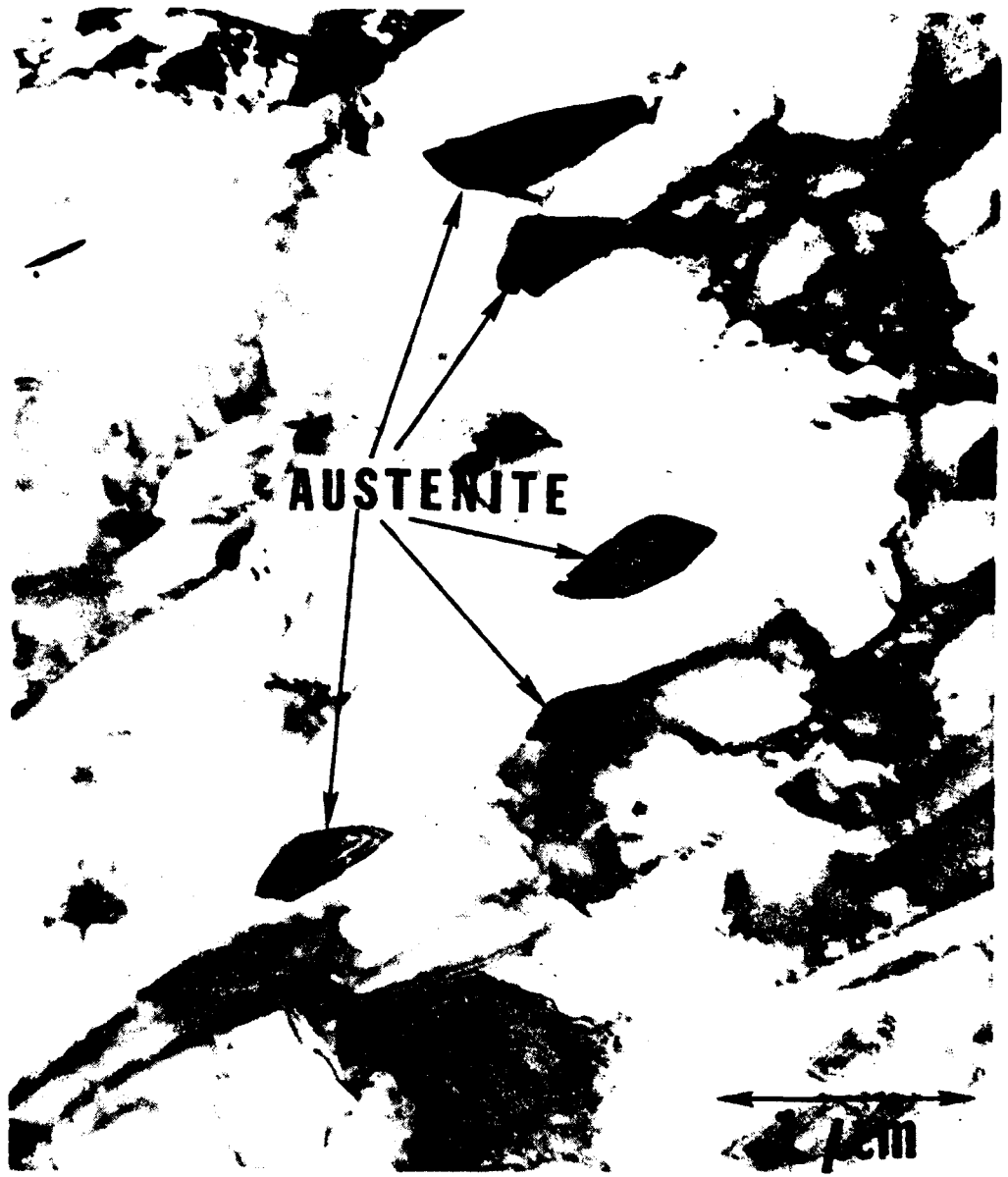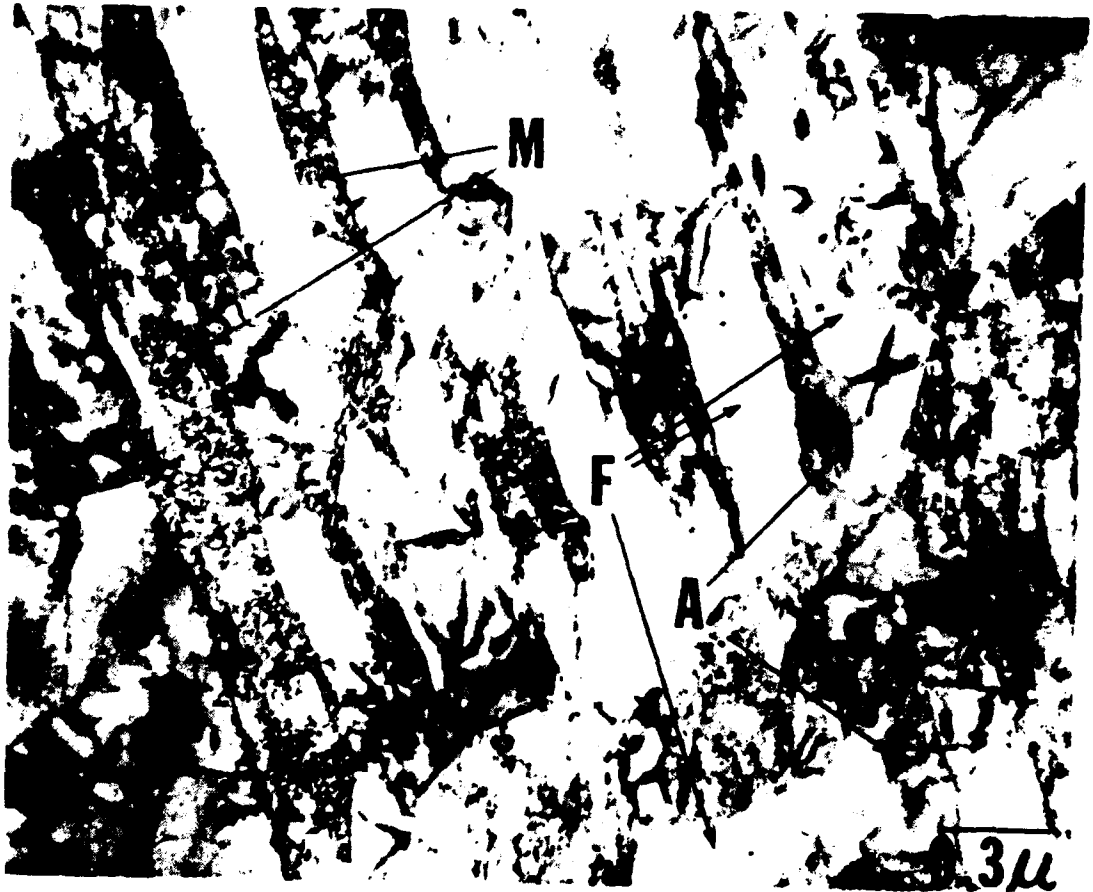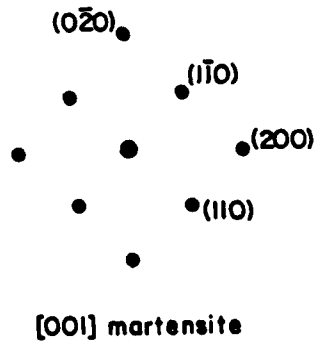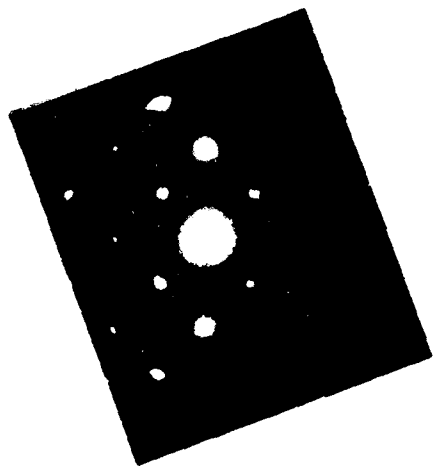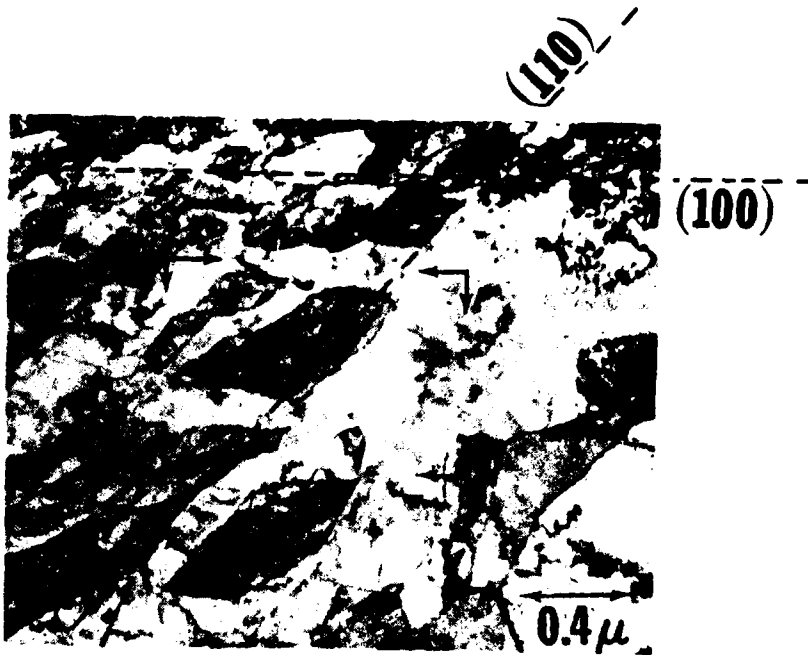
[001] martensite

INTERCRITICALLY ANNEALED

Figure 9

(1̄1̄0)ₘ
(1̄1̄1)γ
(101̄)ₘ
(002)γ
(11̄1̄)γ
(1̄01)ₘ

○ [111] Martensite
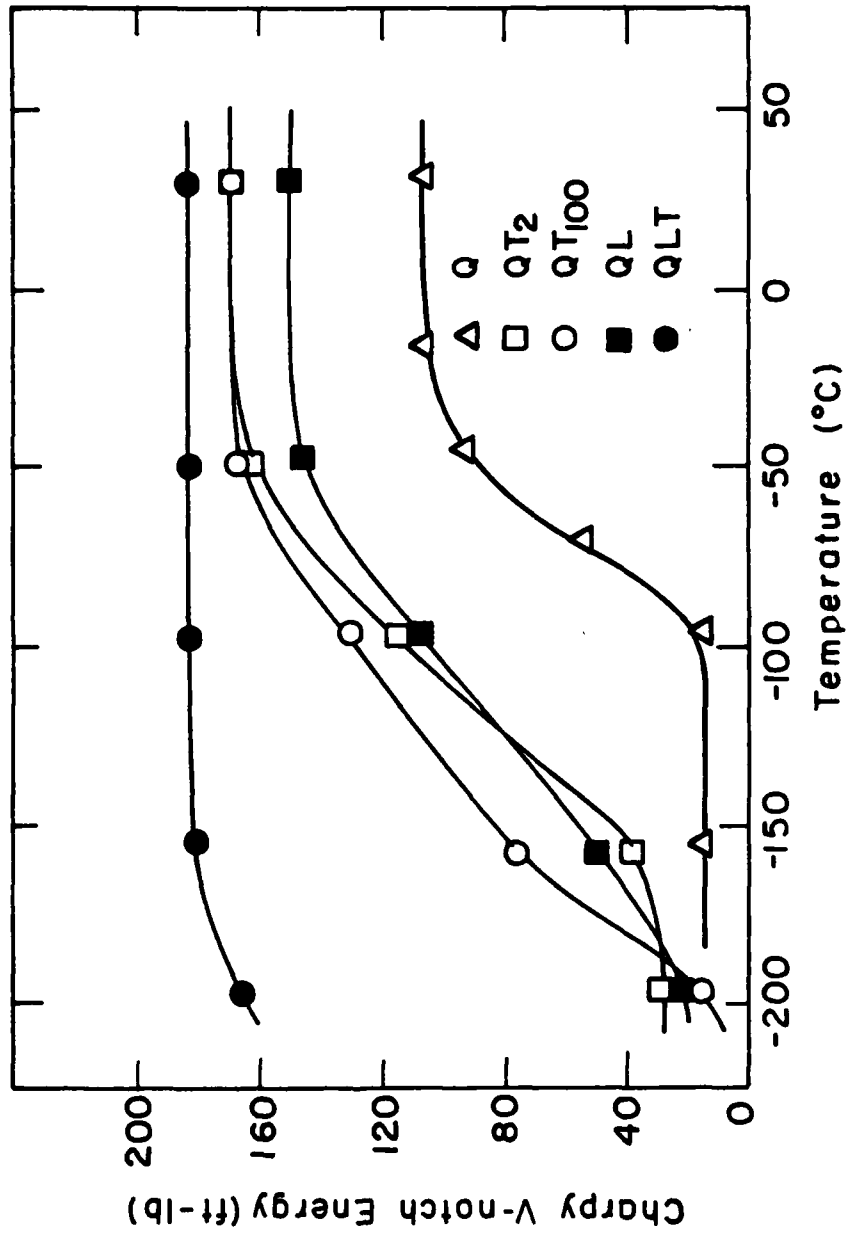● [110] Austenite
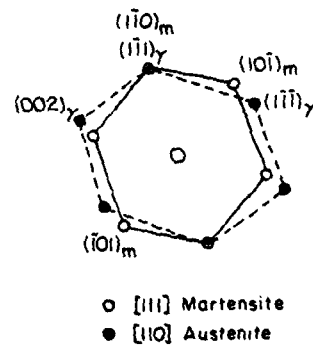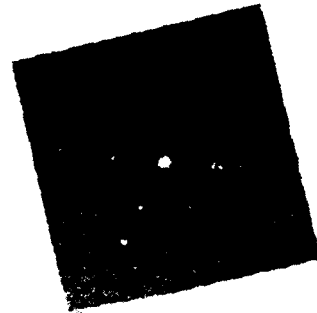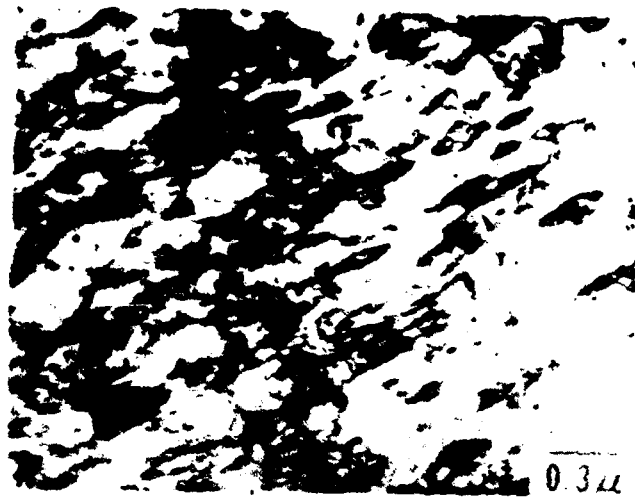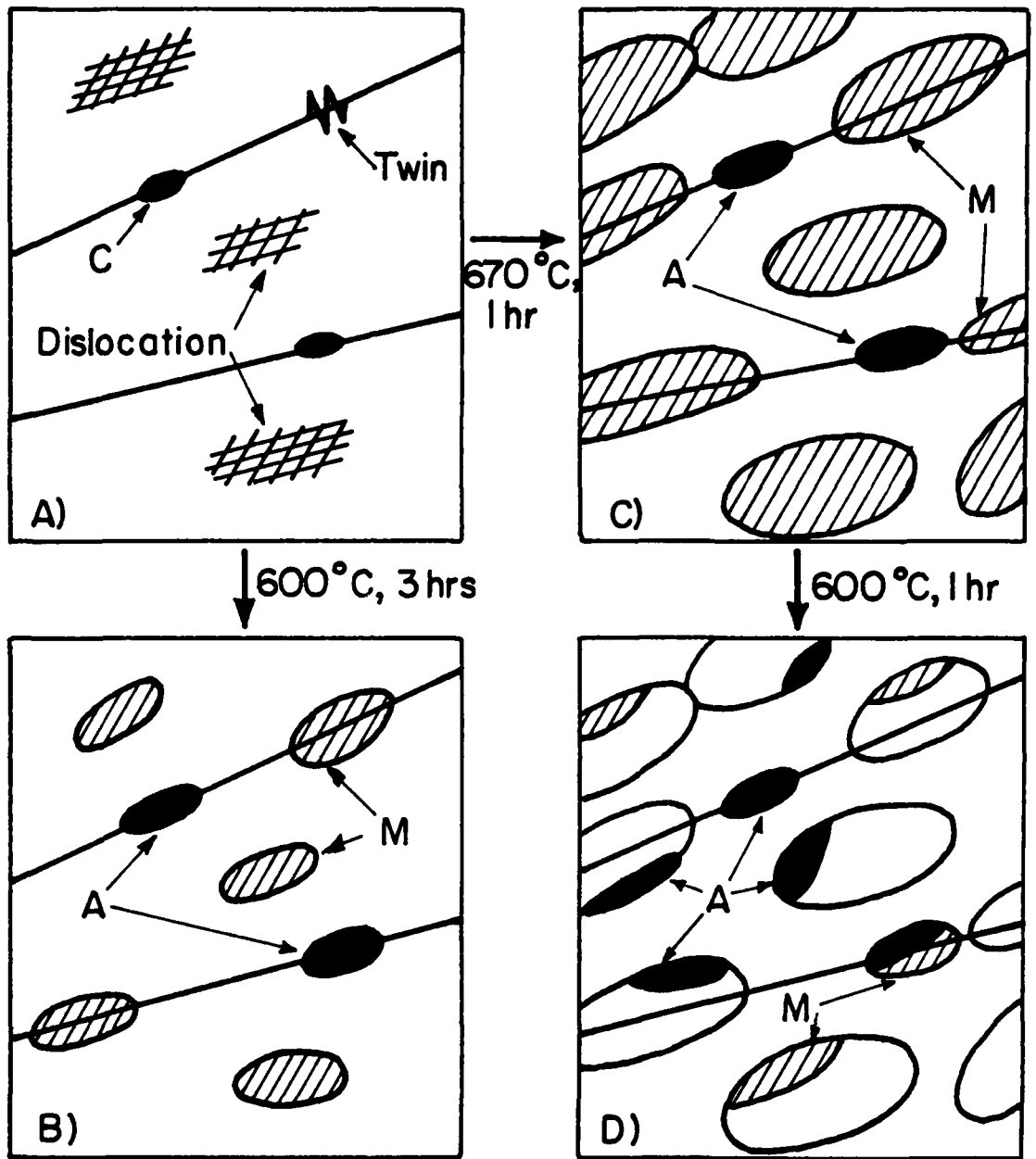
Figure 10

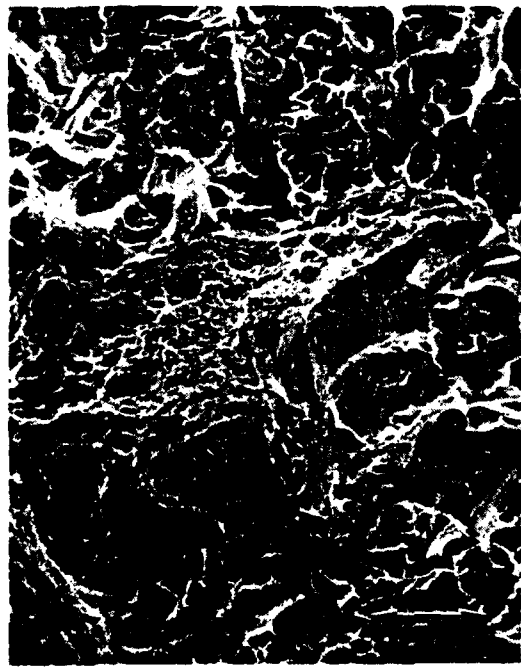Figure 11
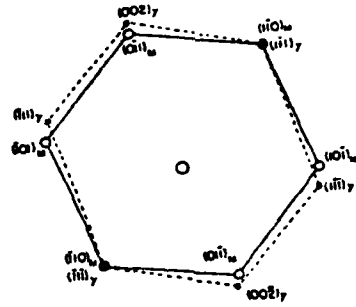
XBL 7910-7191

Figure 12

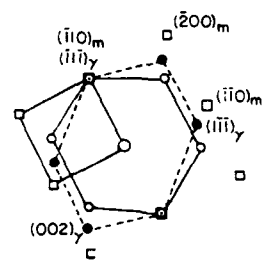XBL 815-5664 A

Figure 13

Figure 14

(a)

(b)

(c)

—○— [III] Martensite Orientation

—●— [110] Austenite Orientation

Figure 15

Figure 16

□ [OOI] Martensite
○ [III] Martensite
● [IIO] Austenite

$(\bar{1}10)_m$
$(\bar{1}1\bar{1})_\gamma$

$(\bar{2}00)_m$

$(\bar{1}\bar{1}0)_m$
$(\bar{1}\bar{1}\bar{1})_\gamma$

(002)